Study of Al^{3+} Binding and Conformational Properties of the Alanine-Substituted C-Terminal Domain of the NF-M Protein and Its Relevance to Alzheimer's Disease†

Z. M. Shen,‡ A. Perczel,‡,§ M. Hollósi,§ I. Nagypál,∥ and G. D. Fasman*,‡

Department of Biochemistry, Brandeis University, Waltham, Massachusetts 02254-9110, Department of Organic Chemistry, Eötvös University, Budapest, H-1117 Hungary, and Department of Physical Chemistry, József Attila University, Szeged, H-6701 Hungary

Received November 4, 1993; Revised Manuscript Received June 7, 1994®

ABSTRACT: NF-M13 [H-(Lys-Ser-Pro-Val-Pro-Lys-Ser-Pro-Val-Glu-Glu-Lys-Gly)-OH], NF-M17 [H-(Glu-Glu-Lys-Gly-Lys-Ser-Pro-Val-Pro-Lys-Ser-Pro-Val-Glu-Glu-Lys-Gly)-OH], and their phosphorylated derivatives, representing the C-terminal phosphorylation domain of the neurofilament protein midsize subunit, have four possible binding sites for metal ions: the COO^- group of glutamate, the OH group of the serine residue, the PO_3H^- group of phosphoserine (when present), and the COO^- at the terminus of the peptide chain. The CD titration of the phosphorylated neurofilament fragments with Al^{3+} and Ca^{2+} yielded a significant conformational change that resulted in conformations containing high β-pleated-sheet contents, which precipitate on standing (intermolecular complex). Al^{3+} binding to the unphosphorylated NF-M13 and NF-M17 did not exhibit this behavior. Several alanine analogues of the parent NF-M17 peptide were synthesized in order to determine the relationship between metal ions and possible binding sites. CD titration of analogues with Ca^{2+} indicated that the critical residues of NF-M17 for Ca^{2+}-induced conformational changes, from random to β-pleated sheet, are the N-terminal serine or both phosphorylated serines. Al^{3+}-induced conformational changes suggest that the critical sites of NF-M17 yielding the β-pleated-sheet structure are the four glutamates or phosphorylated serines, especially the C-terminal SerP. On the basis of the titration data, it is very likely that analogues with a serine in position 11 form a stable intramolecular complex with Al^{3+} that, however, does not result in the adoption of the β-conformation. Back-titration with citric acid fails to reverse the Al^{3+}-induced conformational changes of the phosphorylated peptides. The above results, especially the possible formation of intramolecular and intermolecular Al^{3+} complexes, may have relevance to the molecular mechanism, through which the neurotoxin Al^{3+} gives rise to the formation of neurofilament tangles.

Al^{3+} is generally accepted to be a neurotoxic agent [for an excellent review, see Meiri *et al.* (1993)]. Increased levels of Al^{3+} have mainly been detected in both forms of neuronal lesions, the senile plaques and neurofibrillary tangles (NFTs[1]), characteristic of Alzheimer's disease (AD) and in other Al^{3+}-related neurodegenerative diseases (Doll, 1993; Meiri *et al.*, 1993; Perry, 1990). However, the involvement of Al^{3+} in the etiology of AD is still controversial (Meiri *et al.*, 1993; Doll, 1993). Recently, the importance of the role of Al^{3+} in neurological disorders has been questioned (Landsberg *et al.*, 1992) because the initial event(s) involving the participation of Al^{3+} has not been unambiguously established.

The major and most frequent change of the neuronal cytoskeleton upon exposure to Al^{3+} is the abnormal accumulation of single 10-nm-thick neurofilaments (Crapper-McLachlan, 1986; Crapper-McLachlan & Van Berkum, 1986; Wisniewski *et al.*, 1966; Klatzo *et al.*, 1965; Terry & Pena, 1965). These filaments show resemblance to the NFTs characteristic of AD (Crapper-McLachlan & Van Berkum, 1986), but electron microscopic studies indicate that the neurofilamentous deformations induced by exposure to Al^{3+} compounds are not identical to the paired helical filaments (PHFs) characteristic of NFTs in the diseased human brain (Terry, 1983; Crapper & Dalton, 1973; Terry & Pena, 1965).

The dense neurofilament masses found in the brains of Al^{3+}-treated animals are composed of constituents of the normal neurofilament protein triplet including NF-L (65 kDa), NF-M

† This research was supported by a grant from the NIH (R01-AG10002), a grant from The Hungarian Scientific Research Foundation (OTKA III 2239), and a joint grant from the NSF and Hungarian Academy of Sciences. G.D.F. is the Rosenfield Professor of Biochemistry.

* Author to whom correspondence should be addressed.
‡ Brandeis University.
§ Eötvös University.
∥ József Attila University.

® Abstract published in *Advance ACS Abstracts*, July 15, 1994.

[1] Abbreviations: AD, Alzheimer's disease; APP, amyloid precursor protein; NFT, neurofibrillary tangle; CD, circular dichroism; HPLC, high-pressure liquid chromatography; TFA, trifluoroacetic acid; TFE, 2,2,2-trifluoroethanol; $r_{Ca} = [Ca^{2+}]/[peptide]$; $r_{Al} = [Al^{3+}]/[peptide]$; NF-M17, (EEKG)-NF-M13, where NF-M13 (KSPVPKSPVEEKG) is from a C-terminal repeating 13-mer sequence of an NF-M subunit of human neurofilaments; NF-M17($S^6PS^{11}P$), NF-M17 with $Ser(PO_3H_2)$ replacing Ser at 6 and 11; NF-M17(A^6A^{11}), NF-M17 with Ala replacing Ser at 6 and 11; NF-M17(A^6), NF-M17 with Ala replacing Ser at 6; NF-M17($A^6S^{11}P$), NF-M17(A^6) with $Ser(PO_3H_2)$ replacing Ser at 11; NF-M17(A^{11}), NF-M17 with Ala replacing Ser at 11; NF-M17(S^6PA^{11}), NF-M17(A^{11}) with $Ser(PO_3H_2)$ replacing Ser at 6; NF-M17($A^1A^2A^{14}A^{15}$), NF-M17 with Ala replacing Glu at each position indicated; NF-M17($A^1A^2A^{14}A^{15}S^6P$), NF-M17($A^1A^2A^{14}A^{15}$) with $Ser(PO_3H_2)$ replacing Ser at 6; NF-M17($A^1A^2A^{14}A^{15}S^{11}P$), NF-M17($A^1A^2A^{14}A^{15}$) with $Ser(PO_3H_2)$ replacing Ser at 11; NF-M17($A^1A^2A^{14}A^{15}S^6PS^{11}P$), NF-M17($A^1A^2A^{14}A^{15}$) with $Ser(PO_3H_2)$ replacing Ser at 6 and 11; NF-M17($A^1A^2A^{11}A^{14}A^{15}$), NF-M17($A^1A^2A^{14}A^{15}$) with Ala replacing Ser at 11; NF-M17($A^1A^2A^6A^{14}A^{15}$), NF-M17($A^1A^2A^{14}A^{15}$) with Ala replacing Ser at 6; I, initial conformation; β, β-pleated-sheet dominated conformation; M, mixture of conformers or conformational regions; R, random (aperiodic or unordered) dominated conformation; M(R) and M(β), spectra reflect shifts to the random or β-conformation; M(I), small conformational change. For abbreviated formulas, see Table 1.

0006-2960/94/0433-9627$04.50/0

(160 kDa), and NF-H (200 kDa) molecular mass subunits (Selkoe *et al.*, 1979). A mechanism for the induction of neurofilament (NF) bundling by Al^{3+} ions has been suggested recently (Leterrier *et al.*, 1992). According to *in vitro* experiments presented by these authors, Al^{3+} alone, or in combination with maltol or other chelators, increases the phosphorylation of NF-M and NF-H subunits and induces the aggregation of NFs. A crucial point of this hypothetical mechanism is the chemical nature of the Al^{3+}-binding sites on the NF molecules. Interestingly, an acidic domain of the amyloid precursor protein (APP) exists that shares sequential similarities with the three NF subunits (Delamarche, 1989). APP is the precursor of the A4 (β or βA4) peptide or protein, the major component of the amyloid plaques of AD (Selkoe, 1991). This conserved acidic domain may serve as a binding site for the multivalent "natural" cations Mg^{2+} and Ca^{2+} and also for the neurotoxic cation Al^{3+}. The Ca^{2+} ion plays a central role in the regulation of important neuronal processes (Kennedy, 1989). It is also involved in the phosphorylation of APP, which may have an influence on the proteolysis of APP and thereby on the deposition of plaques (Saito *et al.*, 1993). Abnormal calcium metabolism has been suggested to play a role in both aging and AD (Khachaturian, 1989).

The human NF-M protein contains a 13-mer sequence, KSPVPKSPVEEKG (NF-M13), that is repeated contiguously six times near the C-terminus (tail region of the protein) (Myers *et al.*, 1987). The tetramer KSPV, repeated 12 times in this domain, was found to be the C-terminal repeating phosphorylation site of NF-M (Tokutake, 1990; Geisler *et al.*, 1983). The microtubule-associated protein τ, the main proteinous component of NFTs, appears to acquire Alzheimer-like properties upon phosphorylation with a specific brain kinase (Biernat *et al.*, 1992). One of the potential phosphorylation sites of τ (KSPV) is identical with the repeating phosphorylation site of NF-M.

Phosphorylation of one or both serines in peptides representing the repeating C-terminal domain of NF-M yields derivatives that possess three types of potential binding sites: COO^-, PO_3H^- of phosphoserine, and OH of serine. In the unphosphorylated and double-phosphorylated NF peptides, only two differential binding sites are present.

The results of our circular dichroism (CD) and Fourier transform infrared (FT-IR) studies on peptides and phosphopeptides representing the repeating C-terminal domain of NF-M have been reported in a series of papers (Holly *et al.*, 1993; Hollósi *et al.*, 1992, 1993; Ötvös *et al.*, 1988). Titration of NF-M13 and NF-M17 derivatives in trifluoroethanol (TFE), a low dielectric constant solvent, with Ca^{2+} and Al^{3+} ions has shown that at a certain structure-dependent excess of cations, a significant conformational change occurs. TFE was used to simulate the low dielectric constant of the inner region of neurons. The phosphopeptides, and segments of the unphosphorylated peptides, adopted conformations with a partial, but relatively high (40–90%) β-pleated-sheet content, which precipitated on standing. The cation sensitivity of the peptides was shown to depend on the cation and the number and position of the phosphoryl groups, as well as on the structure of the molecule (Hollósi *et al.*, 1992, 1993). The adoption of the β-pleated-sheet conformation and the aggregation of β-chains in NF-M17(S^6P) and -($S^{11}P$) were also found by FT-IR experiments (Holly *et al.*, 1993). An interesting finding of the cation-binding studies was that the Al^{3+}-induced β-pleated-sheet conformation cannot be reversed by adding citric acid, an excellent Al^{3+} chelator (Martin, 1986), to the Al^{3+} complex of the peptides or phosphopeptides in TFE. Ca^{2+} ions were also found to cause a transition toward the β-pleated-sheet conformation, but this effect could be completely reversed by citric acid.

The aim of this study was to characterize the cation-binding efficiency and β-pleated-sheet-forming tendency of phosphorylated and unphosphorylated NF-M13 and NF-M17 peptides and their analogues in which the glutamates, or one or both of the serine residues, were replaced by alanine (Table 1).

MATERIALS AND METHODS

(a) Synthesis and Purification of Peptides. Peptides were synthesized by the solid-phase technique on a BioSearch SAM II automatic peptide synthesizer using the Fmoc N-terminal-protecting strategy and Fmoc-L-amino acid PAC supports (Fields & Noble, 1990). All amino acid derivatives were purchased from Millipore. The reagents used for peptide synthesis were from Aldrich. The peptides were cleaved from the resin, deprotected using 90% TFA, 5% thioanisole, 3% ethanedithiol, and 2% anisole for 8 h at 20 °C, precipitated, and washed repeatedly with diethyl ether. The peptide phosphorylation was accomplished as described by Ötvös *et al.* (1990).

(b) Purification. The crude peptides and their derivatives were purified by reverse-phase HPLC (Model 420, Beckman) using acetonitrile (solvent B) and water (solvent A) containing 0.1% TFA on a C_{18} column (5 μm, 10 × 250 mm, Beckman) at 3 mL/min. The peptides were analyzed by FAB-mass spectrometry (MIT Mass Spectrum Facility) and amino acid analysis and were found to be pure. The separation yielded a k' value (Table 2). k' was calculated as usual by $k' = (t - t_0)/t$, where t is the time of appearance of the peptide and t_0 is the time of appearance of the solvent peak. The gradient of HPLC was as follows: 0–5 min 0–11% B, 5–25 min 11–15% B, 25–28 min 15–100% B for crude NF-M13; 0–2 min 0% B, 2–7 min 0–8% B, 7–29 min 8–14% B, 29–32 min 14–100% B for phosphorylated NF-M13 peptides.

(c) Circular Dichroism. CD spectra were recorded on a Jobin Yvon dichrograph Mark V, as described by Prevelige and Fasman (1992). NMR-grade TFE (Aldrich), $Ca(ClO_4)_2 \cdot H_2O$ (22.2% H_2O, Alfa), citric acid hydrate (Fischer), and $Al(ClO_4)_3 \cdot 9H_2O$ (Aldrich) were used. Peptide concentrations of samples were 0.1–0.5 mg/mL. $[\theta]_M$, the mean residue ellipticity, is given in deg·cm^2/dmol. The CD data were analyzed by the Lincomb algorithm (Perczel *et al.*, 1992). The Lincomb algorithm is based on a least-squares fit, with a set of reference globular protein spectra that was obtained from the deconvolution of 25 proteins with known secondary structure. The calculated secondary structure was an estimation of weights attributed to α-helix, β-sheet (mainly antiparallel), β-turn, unordered, and aromatic/disulfide (or nonpeptide) contributions.

(d) Ca^{2+} Binding Analysis. The stability constants of calcium complexes of citric acid and NF-M13(S^2P) were measured potentiometrically using a Ca^{2+}-selective electrode (Model 93-20, Orion Research, Inc., Boston, MA), with an Ag/AgCl reference electrode. The samples were dissolved in a 0.1 M borate buffer at pH 7.3 or 9.15. Electrode calibrations were performed prior to titration of the samples. The data were analyzed as described by Zékány and Nagypál (1985).

(e) Analysis of Peptides. All peptides were characterized by amino acid analysis and positive ion FAB-MS (Ötvös *et al.*, 1990): e.g., NF-M13, MS 1381.9, calcd 1389.9 Da; NF-M17, MS 1501.8 calcd 1500.8 Da; NF-M17(A^6S^{11}) found in mole %: Glu 22.1%, Ser 5.9%, Gly 12.8%, Pro 16.8%, Val

Table 1: Circular Dichroism Spectra of NF-M17 and Ala Analogues in TFE

peptide abbrev	model	conformational change based on CD spectra[a]	[metal ion]/[peptide] ratio	CD parameters in TFE: nπ* band λ (nm)	nπ* band [θ]m	ππ* bands λ (nm)	ππ* bands [θ]m	ππ* bands λ (nm)	ππ* bands [θ]m
NF-M17	^{1}EEKG^{5}KSPVP^{10}KSPVE^{15}EKG		no metal ion	220	−3200	203	−5000	185	5000
			[Ca]/[pep] = 2	220	−3200	205[c]	−2000	188	6500
		I→β	[Ca]/[pep] = 4	219	−2800	205[c]	−1300	185[b]	3800
		β→I (rev)	[cit]/[Ca] = 4	220	−3000	203	−5000	185	5000
		I→M	[Al]/[pep] = 16	218	−3200	202	−3400	185	3700
		no change	[cit]/[Al] = 8	218	−3100	202	−3200	185	3100
NF-M17(S^{6}PS^{11}P)	EEKGKS(-PO_3H_2)PVPKS(-PO_3H_2)PVEEKG		no metal ion	218	−4500	203	−5000	185	3300
		I→M	[Ca]/[pep] = 16	218	−4000	203[c]	−3300	185	3300
		M→R	[cit]/[Ca] = 16	218	−3000	198	−4100	185	2200
		I→β	[Al]/[pep] = 8	218	−5300	203[b]	−4000	185	5000
		no change	[cit]/[Al] = 16	218	−4900	203[b]	−3600	185	5000
NF-M17(A^{6}A^{11})	EEKGKAPVPKAPVEEKG		no metal ion	221	−3000	200	−4500	185	1300
		I→R	[Ca]/[pep] = 16	221[c]	−2000	196.5	−5600	185	800
		R→I (rev)	[cit]/[Ca] = 16	221	−3000	200	−4700	185	2000
		I→M(β)	[Al]/[pep] = 16	216	−4200	200[b]	−2700	185	2700
		no change	[cit]/[Al] = 8	218	−3300	200	−2900	185	2500
NF-M17(A^{6})	EEKGKAPVPKSPVEEKG		no metal ion	218	−3000	201.5	−4300	185[b]	2100
		I→R	[Ca]/[pep] = 16	216	−1850	196	−4000	185[b]	2100
		R→I (rev)	[cit]/[Ca] = 16	218	−2800	201	−4300	185[b]	2100
		I→M	[Al]/[pep] = 16	215[c]	−4100	201.5[c]	−4000	185[c]	3100
		no change	[cit]/[Al] = 12	216	−3950	201.5	−3900	185[c]	3100
NF-M17(A^{6}S^{11}P)	EEKGKAPVPKS(-PO_3H_2)PVEEKG		no metal ion	218	−3000	205	−3400	186	2200
		I→M(R)	[Ca]/[pep] = 16	216[c]	−2800	200	−3400	186	3000
		M(R)→I	[cit]/[Ca] = 16	218	−3000	196	−6100	186[c]	1500
		I→M(β)	[Al]/[pep] = 16	218	−4250	205[c]	−3500	186	4500
		M(β)→M	[cit]/[Al] = 16	218	−3300	205[c]	−2400	186	6000
NF-M17(A^{11})	EEKGKSPVPKAPVEEKG		no metal ion	218	−3800	200	−6300	186	1900
		I→M	[Ca]/[pep] = 16	218	−3400	197	−4800	186[b]	3500
		M→I (rev)	[cit]/[Ca] = 16	218	−3600	199.5	−6500	186	3000
		I→M(β)	[Al]/[pep] = 16	218	−4600	200	−5300	186	2000
		M(β)→M	[cit]/[Al] = 4	218	−4500	201	−4800	186	3500
NF-M17(S^{6}PA^{11})	EEKGKS(-PO_3H_2)PVPKAPVEEKG		no metal ion	218	−3300	200	−4900	186	1800
		I→β	[Ca]/[pep] = 16	218	−3200	200[c]	−2900	187	3000
		β→I (rev)	[cit]/[Ca] = 16	218	−3100	200	−4900	186	2400
		I→M(β)	[Al]/[pep] = 16	218	−4100	200[c]	−3000	186	2000
		M(β)→M	[cit]/[Al] = 16	218	−3500	200[c]	−2000	186	4000
NF-M17(A^{1}A^{2}A^{14}A^{15})	AAKGKSPVPKSPVAAKG		no metal ion	220[c]	−3200	201	−6000	185[b]	1500
			[Ca]/[pep] = 2	220	−3200	202[b]	0	192	3800
		I→β	[Ca]/[pep] = 3	220	−2400	201[b]	0	192	2000
		β→I (rev)	[cit]/[Ca] = 2	220[c]	−3000	200	−5700	185[b]	2000
		I→M(R)	[Al]/[pep] = 8	220[c]	−2200	197	−4900	185[b]	0
		M(R)→M	[cit]/[Al] = 16	220[c]	−3000	202	−4600	185[b]	2200
NF-M17(A^{1}A^{2}A^{14}A^{15}S^{6}P)	AAKGKS(-PO_3H_2)PVPKSPVAAKG		no metal ion	220	−2500	200	−4700	185[b]	3500
		I→M	[Ca]/[pep] = 16	220	−2300	200	−5200	185[b]	4400
		no change	[Al]/[pep] = 8	220	−2200	199	−4500	185[b]	3500
		no change	[cit]/[Al] = 8	220	−2500	201	−4500	185[b]	3500
NF-M17(A^{1}A^{2}A^{14}A^{15})S^{11}P)	AAKGKSPVPKS(-PO_3H_2)PVAAKG		no metal ion	219	−3000	199	−4300	185[b]	800
		I→M	[Ca]/[pep] = 16	219	−1200	199	−2100	185[b]	800
		M(R)	[cit]/[Ca] = 16	219	−2600	199	−4700	185[b]	3500
		I→M(I)	[Al]/[pep] = 14	219	−3200	201	−3800	185[b]	1100
		no change	[cit]/[Al] = 8	219	−3100	202	−3300	185[b]	2600
NF-M17(A^{1}A^{2}A^{14}A^{15}S^{6}PS^{11}P)	AAKGKS(-PO_3H_2)PVPKSPVAAKG		no metal ion	219	−3400	201	−4900	185[b]	1000
		I→M(β)	[Ca]/[pep] = 8	219	−2200	201	−700	188	1000
		M(β)→M(R)	[cit]/[Ca] = 8	219	−2200	201	−3800	188[b]	1000
		I→M	[Al]/[pep] = 8	220	−3400	201	−3500	185[b]	1200
		no change	[cit]/[Al] = 16	219	−3400	201	−3500	185[b]	1200

[a] The same conformational changes were observed at lower [cation]/[pep] and [cit]/[cation] ratios. I, initial conformation; β, β-pleated-sheet dominated conformation; M, mixture of conformers or conformational regions; R, random (aperiodic or unordered) dominated conformation; M(R) and M(β), spectra reflect shifts to random or β-conformation; M(I), small conformational change. [b] No band. [c] Shoulder.

Table 2: k' Values of the Purification of NF-M13 and Its Phosphorylated Fragments on HPLC[a]

	NF-M13-(S^{2}PS^{7}P)	NF-M13-(S^{7}P)	NF-M13-(S^{2}P)	NF-M13 (nonphosphorylated)
$k' = (t - t_0)/t_0$	2.86	3.79	4.24	4.90

[a] t = time of peak appearance of the peptide; t_0 = time of solvent peak appearance.

10.9%, Lys 22.2%; calcd: Glu 23.5%, Ser 5.9%, Gly 12.8%, Pro 16.8%, Val 17.7%, Lys 22.2%.

RESULTS AND DISCUSSION

(a) Ca^{2+} and Al^{3+} Titration and Citric Acid Back-Titration of Nonphosphorylated NF-M13 and NF-M17. CD titration of unphosphorylated NF-M13 or NF-M17 in TFE with Ca^{2+} induced a conformational change from random coil to β-sheet (see, for example, Figure 1 and supplementary material Figure 3B). [For preliminary data, see Hollósi *et al.* (1992, 1993).] The intensity of the negative trough near 205 nm decreased with the increase in the $[Ca^{2+}]/[pep]$ ratio (r_{Ca}). At r_{Ca} =

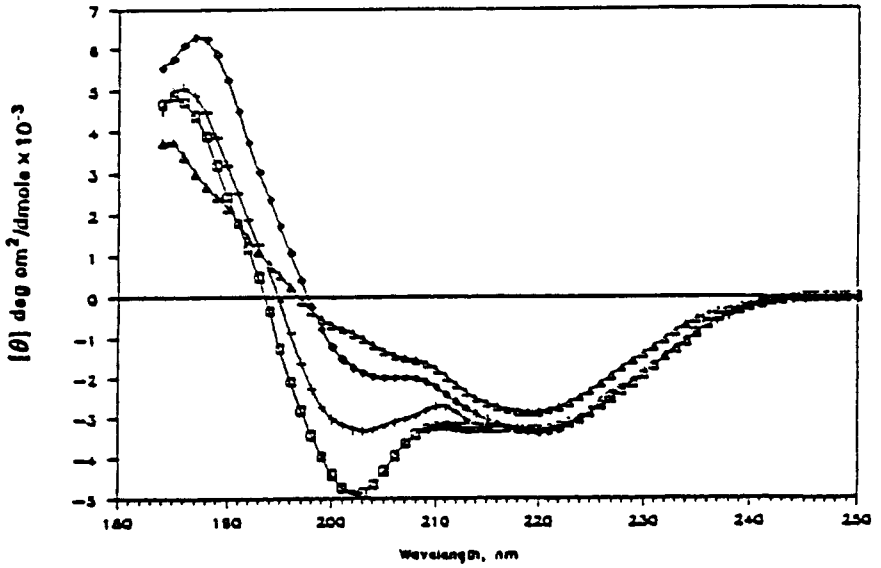

FIGURE 1: Circular dichroism titration of NF-M17 in TFE with Ca^{2+}: □, no Ca^{2+}; +, $[Ca^{2+}]/[pep] = 1$; ◇, $[Ca^{2+}]/[pep] = 2$; △, $[Ca^{2+}]/[pep] = 4$; [pep] = 0.282×10^{-4} M.

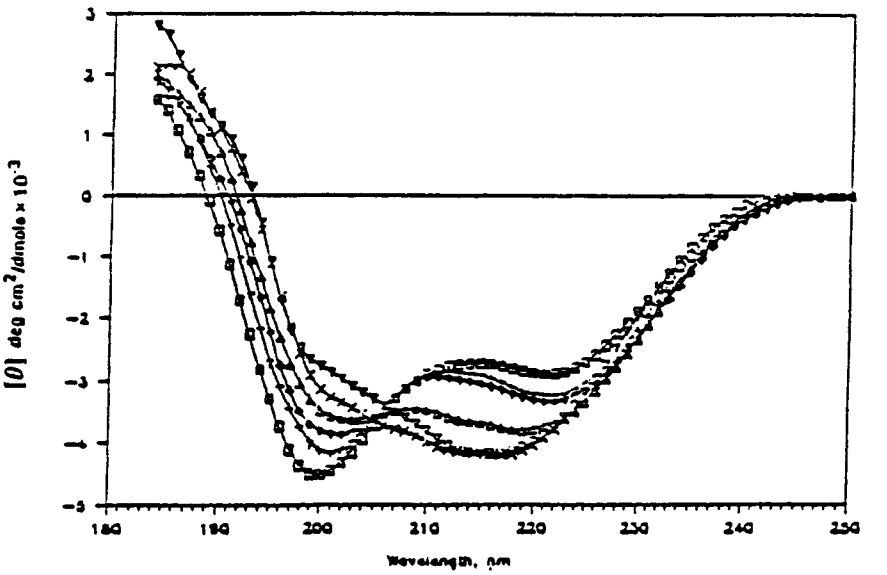

FIGURE 2: Circular dichroism titration of NF-M17 in TFE with Al^{3+}: □, no Al^{3+}; +, $[Al^{3+}]/[pep] = 2$; ◇, $[Al^{3+}]/[pep] = 4$; △, $[Al^{3+}]/[pep] = 8$; ×, $[Al^{3+}]/[pep] = 16$; [pep] = 0.282×10^{-4} M.

2, the 205-nm band almost vanished, the 220-nm trough did not change, and the positive band shifted to ~190 nm. The Ca^{2+}-induced conformational change of NF-M13, from random coil to β-sheet, was reversible with back-titration with citric acid (supplementary material Figure 3B).

In the presence of Al^{3+}, until the $[Al^{3+}]/[pep]$ (r_{Al}) ratio increased to 4, the CD titrations of NF-M13 and NF-M17 showed much smaller conformational changes than were induced by Ca^{2+} (Figure 2; supplementary material Figure 2B,C). At $r_{Al} = 1$, the CD spectrum was similar to the original spectrum without Al^{3+}. Even at $r_{Al} = 4$, the intensities of all three bands did not change significantly. The spectral effect of Al^{3+} was not reversed by citric acid (Figure 4; supplementary material, Figure 4B–D).

(b) Ca^{2+} Titration and Citric Acid Back-Titration of Phosphorylated NF-M13 and NF-M17. CD titration curves of different phosphorylated species of NF-M13 (S^2P, S^7P, and S^2PS^7P) (Scheme 1) in TFE with Ca^{2+}, at r_{Ca} between 0 and 12, showed a typical conformational change. For phosphorylated NF-M17 peptides, similar spectral effects

Scheme 1: Amino Acid Sequences and Abbreviated Names of Peptides and Phosphopeptides Representing the C-Terminal Repeating Domain of the Neurofilament Protein Mid-Sized Subunit (NF-M)

K S P V P K S P V E E K G	NF-M13
K $\overset{2}{S}$ P V P K S P V E E K G | (PO_3H_2)	NF-M13 (Ser^2P)
K S P V P K $\overset{7}{S}$ P V E E K G | (PO_3H_2)	NF-M13 (Ser^7P)
K $\overset{2}{S}$ P V P K $\overset{7}{S}$ K P V E E K G | | (PO_3H_2) (PO_3H_2)	NF-M13 (Ser^2PSer^7P)

previously had been attributed to a shift from random coil to a β-sheet structure (Hollósi *et al.*, 1992). At $r_{Ca} = 0.5$, a small spectral change was observed; at ratios between 1.5 and 6, the spectra shifted gradually and showed increasingly more β-sheet character. In the case of monophosphopeptides, the

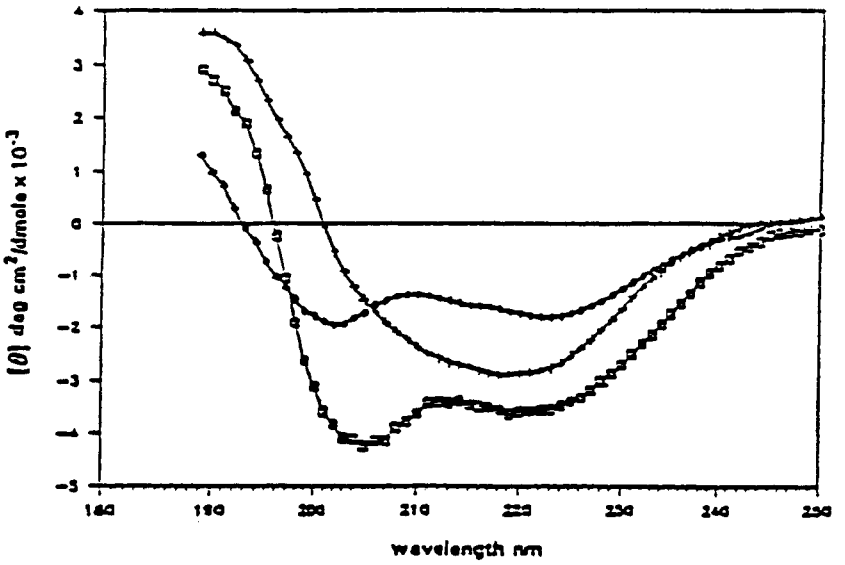

FIGURE 3: Citric acid back-titration experiments on the Ca^{2+} complex NF-M13(S^2PS^7P) in TFE: [pep] = 2.17×10^{-4} M; □, no Ca^{2+} or citric acid; +, $[Ca^{2+}]/[pep] = 12$; ◇, $r_{Ca} = 12$ and $[cit]/[Ca^{2+}] = 8$; concentration as in Figure 1.

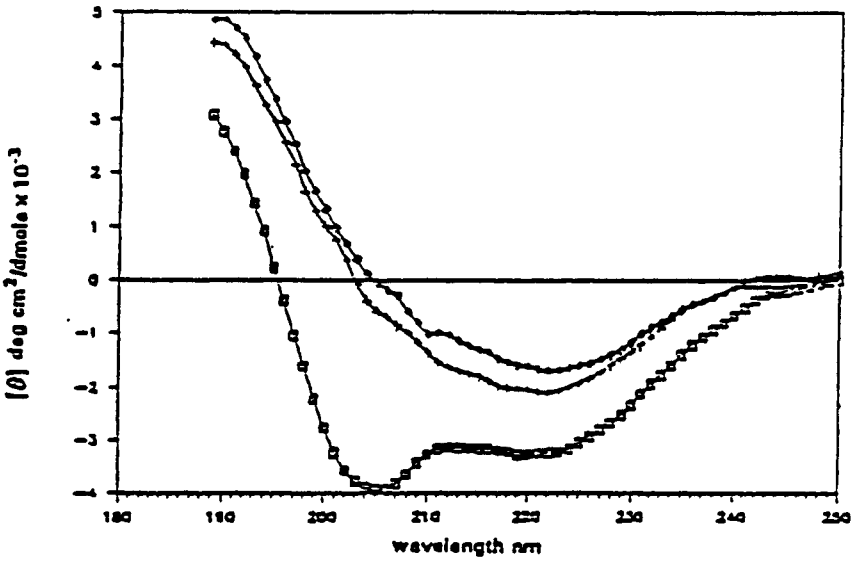

FIGURE 4: Citric acid back-titration experiments on the Al^{3+} complex NF-M13(S^2PS^7P) in TFE: [pep] = 2.17×10^{-4} M; □, no Al^{3+} or citric acid; +, $[Al^{3+}]/[pep] = 12$; ◇, $r_{Al} = 12$ and $[cit]/[Al^{3+}] = 4$; concentration as in Figure 2.

spectral transition was completed at about $r_{Ca} = 6$, while the diphosphorylated peptides showed a slower spectral change, with definite changes between a 6 and 12 times excess of Ca^{2+}. The NF-M13(S^2P) and NF-M13(S^7P) peptides, with increases in Ca^{2+}, yielded a decrease in the intensity of the band at 205 nm, as well as a minor intensity change near 220 nm (Figure 3; supplementary material Figures 3C,D and 4D). The spectra of the diphosphorylated NF-M13 peptide between $r_{Ca} = 0.5$ and 6 were blue shifted with an intensity decrease (not shown). At $r_{ca} = 12$, the blue-shifted 205-nm peak disappeared, and the conformational change yielded more β-sheet structure (Figure 3).

The Ca^{2+} complexes of the phosphorylated NF-M13 and NF-M17 peptides were dissociated upon the addition of citric acid (see Figure 3; supplementary material Figure 3C,D); however, in the presence of citric acid, the measured spectra showed characteristic differences relative to the spectra of the parent peptide (without Ca^{2+} and citric acid). For the conformational changes induced by the cations and citric acid, see Table 1.

(c) Al^{3+} Titration and Citric Acid Back-Titration of Phosphorylated NF-M13 and NF-M17. In agreement with the data reported for the phosphorylated NF-M17 peptides (Hollósi *et al.*, 1992), the Al^{3+} titration of the various phosphorylated NF-M13's showed spectral changes that were similar to those induced by Ca^{2+} ions (Figure 4; supplementary material, Figure 4B–D). On the basis of a comparison of the CD titration data, Al^{3+} is superior to Ca^{2+} in inducing a spectral change, reflecting the adoption of the β-sheet conformation.

Al^{3+}-induced conformational changes of the phosphorylated NF-M13 peptides, from random coil to a β-pleated-sheet structure, were not reversed with back titration with citric acid (Figure 4; supplementary material Figure 4C,D). The original spectra were not recovered in the case of NF-M13 and NF-M13(S^7P), but upon the addition of citric acid, the spectra showed definite changes (supplementary material Figure 4B–D). A similar nonreversibility, upon the addition of citric acid, was also observed for the phosphorylated NF-M17 peptides (Table 1).

(d) Ca^{2+}- and Al^{3+}-Induced Conformation Transitions of Alanine-Substituted Unphosphorylated Fragments. CD-

Table 3: Secondary Structure of NF-M17 Ala Analogues with Ca^{2+} and Al^{3+} and Their Reversibility with Citric Acid

peptide abbrev	[metal ion]/[peptide] or [citric acid]/[metal ion] ratio	α-helix (%)	β-sheet (%)	random (%)	error/46 points
NF-M17	no metal ion	4	36	60	0.45
	[Ca]/[pep] = 2	6	42	52	0.45
	[cit]/[Ca] = 4	4	45	51	0.35
	[Al]/[pep] = 16	3	40	58	0.27
	[cit]/[Al] = 8	4	39	57	0.28
NF-M17($S^6PS^{11}P$)	no metal ion	5	35	60	0.40
	[Ca]/[pep] = 16	5	38	57	0.38
	[cit]/[Ca] = 16	1	42	58	0.30
	[Al]/[pep] = 16	3	47	50	0.35
NF-M17(A^6A^{11})	no metal ion	1	40	60	0.42
	[Ca]/[pep] = 16	0	38	62	0.61
	[cit]/[Ca] = 16	1	39	60	0.33
	[Al]/[pep] = 16	5	39	56	0.03
	[cit]/[Al] = 8	4	40	57	0.22
NF-M17(A^6)	no metal ion	2	39	59	0.48
	[Ca]/[pep] = 16	0	41	59	0.67
	[cit]/[Ca] = 16	1	39	60	0.48
	[Al]/[pep] = 16	4	37	59	0.03
	[cit]/[Al] = 12	4	37	59	0.05
NF-M17($A^6S^{11}P$)	no metal ion	3	40	57	0.35
	[Ca]/[pep] = 16	2	49	59	0.31
	[cit]/[Ca] = 16	0	39	61	0.82
	[Al]/[pep] = 16	5	38	57	0.08
	[cit]/[Al] = 16	5	42	53	0.39
NF-M17(A^{11})	no metal ion	1	36	60	0.14
	[Ca]/[pep] = 16	0	40	60	0.09
	[cit]/[Ca] = 16	1	35	64	0.14
	[Al]/[pep] = 16	2	37	61	0.04
	[cit]/[Al] = 16	3	37	60	0.07
NF-M17(S^6PA^{11})	no metal ion	2	37	61	0.22
	[Ca]/[pep] = 16	3	40	57	0.23
	[cit]/[Ca] = 16	1	37	62	0.35
	[Al]/[pep] = 16	4	39	57	0.07
	[cit]/[Al] = 16	6	41	54	0.35
NF-M17($A^1A^2A^{14}A^{15}S^6P$)	no metal ion	0	40	60	0.63
	[Ca]/[pep] = 16	0	38	62	0.56
	[Al]/[pep] = 8	1	38	61	0.32
	[cit]/[Al] = 8	3	37	60	0.29
NF-M17($A^1A^2A^{14}A^{15}S^{11}P$)	no metal ion	0	40	60	0.25
	[Ca]/[pep] = 16	0	45	55	1.13
	[cit]/[Ca] = 16	0	40	60	0.28
	[Al]/[pep] = 14	2	39	59	0.23
	[cit]/[Al] = 8	3	40	57	0.39
NF-M17($A^1A^2A^{14}A^{15}S^6PS^{11}P$)	no metal ion	2	37	61	0.19
	[Ca]/[pep] = 8	2	46	52	0.63
	[cit]/[Ca] = 8	1	40	59	0.52
	[Al]/[pep] = 8	3	40	58	0.20
	[cit]/[Al] = 16	3	39	58	0.24
NF-M17($A^1A^2A^6A^{14}A^{15}$)	no metal ion	1	36	63	0.18
	[Ca]/[pep] = 4	3	45	52	1.75
	[Ca]/[pep] = 16	0	59	41	1.60
	[cit]/[Ca] = 4	1	35	64	0.25
	[Al]/[pep] = 16	1	41	58	0.21
	[cit]/[Al] = 8	3	37	60	0.25

monitored Ca^{2+}- and Al^{3+}-binding studies were performed on NF-M17 and its alanine-substituted unphosphorylated analogues NF-M17(A^6A^{11}) and NF-M17($A^1A^2A^{14}A^{15}$). Ca^{2+} and Al^{3+} had strikingly different spectral effects on the serine- and glutamate-substituted peptides. In the case of NF-M17 and NF-M17($A^1A^2A^{14}A^{15}$), the addition of Ca^{2+} ions at $r_{Ca} > 2$ resulted in significant increases in the β-pleated-sheet conformer populations (Figure 1 and Table 3). The spectra changed gradually, but at $r_{Ca} > 4$, the intensities of both the negative and positive bands began to decrease due to precipitation of the complex and the concomitant concentration decrease in the solution. [Similar behavior was observed earlier and is reported in Holly *et al.* (1993) and Hollósi *et al.* (1992).] The β-pleated-sheet content was calculated to be more than 40% at a ratio of 2 (Table 3). The increase in β-content was accompanied by a comparable decrease in the random conformation.

Upon the addition of Al^{3+} ions, NF-M13, NF-M17, and NF-M17($A^1A^2A^{14}A^{15}$) failed to yield β-pleated-sheet spectra, even at $r_{Al} \geq 8$ (Figure 2; supplementary material Figure 4B–D). The spectrum of the $A^1A^2A^{14}A^{15}$ analogue reflected increasing amounts of random conformation (~50% at $r_{Al} = 8$). According to the CD curve deconvolution data listed in Table 3, all peptides and phosphopeptides used in this study feature a β-pleated-sheet/unordered type conformation, a finding that is supported by FT-IR measurements on phosphorylated NF-M17 fragments (Holly *et al.*, 1993).

The alanine-substituted serine peptide NF-M17(A^6A^{11}) behaved differently upon the addition of Ca^{2+} and Al^{3+} ions. Between $r = 8$ and $r = 16$, the spectral changes became smaller.

The calculated random coil content at r_{Ca} = 16 was 62%, which is only slightly larger than that calculated from the original curve. In contrast, Al^{3+} binding by the A^6A^{11} analogue leads to gradual shifts toward β-pleated-sheet spectra (Figure 2), a trend exhibited upon the addition of Ca^{2+} ions to NF-M13, NF-M17, and NF-M17($A^1A^2A^{14}A^{15}$), but not to NF-M17(A^6A^{11}) (Figure 1). Apparently, Ca^{2+} binding to the carboxylate ligands of glutamate does not play a significant conformational role (Figure 1). By contrast, Al^{3+} binding appears to cause a shift toward the β-pleated sheet only in the case of NF-M17(A^6A^{11}) containing carboxylate but no hydroxy side-chain groups (Figure 2).

The ligand space of Ca^{2+} and Al^{3+} is different (Bittar *et al.*, 1992). It is surprising, nevertheless, that the Ca^{2+}- and Al^{3+}-induced conformational transitions have quite different mechanisms. At least in the case of NF-M17(A^6A^{11}), the Al^{3+}-induced β-pleated-sheet formation appears to be directly connected with Al^{3+} complexation, probably through Al^{3+} cross-bridges between carboxylates from different molecules. Contrary to this, Ca^{2+} ions do not form β-promoting cross-bridges with the same carboxylate groups.

To characterize the importance of the C- and N-terminal serine residues in cation binding and β-pleated-sheet formation, titration experiments were also performed on the alanine analogues NF-M17(A^6) and NF-M17(A^{11}) (with four glutamates), as well as on NF-M17($A^1A^2A^6A^{14}A^{15}$) and NF-M17($A^1A^2A^{11}A^{14}A^{15}$) (with Ala replacing Ser^6 or Ser^{11} and Glu at each position). Ca^{2+} binding by NF-M17(A^6) or NF-M17(A^{11}) resulted in no clear-cut conformational changes. The spectra, measured at high r_{Ca} values, reflected only small shifts (Table 2). Within this group of models, binding of Ca^{2+} induced the most significant conformational change toward the β-pleated-sheet structure in NF-M17-($A^1A^2A^{11}A^{14}A^{15}$) (with Ser at 6) (Table 2). This suggests that the N-terminal serine is more important than the C-terminal serine for Ca^{2+}-induced β-pleated-sheet formation. Al^{3+} binding at high r_{Al} values yielded subtle spectral transitions (Tables 1 and 3).

(e) Cation-Induced Conformational Transitions of Phosphorylated Alanine-Substituted NF-M17 Fragments. The alanine-substituted monophosphate NF-M17($A^6S^{11}P$) did not show a definite conformational effect in the presence of Ca^{2+} (Tables 1 and 3). This disagrees with earlier results on monophosphorylated NF-M17 derivatives showing position-dependent (6 or 11), but significant, β-pleated-sheet formation upon Ca^{2+} binding at $r_{Ca} > 5$. In the isomeric (S^6PA^{11}) phosphopeptide, Ca^{2+} binding gave rise to some (37–40%) increase in the β-pleated-sheet content.

Al^{3+} was found to be an efficient β-sheet promoter in the case of diphosphate models. A marked conformational change (I→β) was observed for NF-M17($S^6PS^{11}P$) at r_{Al} = 8 (Tables 1 and 3). The $A^6S^{11}P$ and S^6PA^{11} monophosphates showed weak and position-dependent Al^{3+} sensitivity, with a stronger β-pleated-sheet-promoting effect of the latter peptide. The mono- and diphosphorylated NF-M17($A^1A^2A^{14}A^{15}$) peptides also showed low and position-dependent cation sensitivity (Tables 1 and 3).

Citric acid back-titration experiments on alanine-substituted peptides (Figure 5, Table 1) are consistent with our earlier findings, which showed that citric acid is an excellent chelator that can overcome the affinity of unphosphorylated and phosphorylated peptides for Ca^{2+}. In TFE, the Ca^{2+}-induced conformational changes were *reversible*.

In aqueous solution, the stability of the Ca^{2+}·cit complex is relatively low: log K_s = 3.5 in water at 0.15 M ionic strength (Bittar *et al.*, 1992; Martin, 1986), 3.15 at pH 9.15 in 0.1 M aqueous $Na_2B_4O_7$ buffer, or 2.85 at pH 7.3 in the same buffer (adjusted with HCl). NF-M13(S^2P) has a log K_s < 1 with Ca^{2+} in aqueous $Na_2B_4O_7$ buffer at pH 7.3. This suggests that hydrated Ca^{2+} ions have only weak binding affinity for the peptide ligand groups. Contrary to this, Al^{3+}-induced conformational changes were not affected by the addition of citric acid. In TFE, complexation of Al^{3+} ions gave rise to transitions toward the β-pleated-sheet conformation in the case of NF-M17(A^6A^{11}) (Figure 2A) and NF-M17($S^6PS^{11}P$) (Table 1). NF-M17(A^{11}) still showed some β-pleated-sheet formation, but the other models listed in Table 1 resulted in no definite spectral changes toward β-sheet (I→β). Most importantly, the effect of Al^{3+} ions could not be reversed by citric acid, regardless of the type of conformation induced. The consistent failure to adopt the β-pleated-sheet conformation by peptides featuring a C-terminal *serine* residue (in position 7 in the 13-mer and position 11 in the 17-mer, respectively) strongly emphasizes the role of the OH function of serine(s) in a type of Al^{3+} complexation that does not lead to the β-pleated-sheet conformation.

Citrate binding of Al^{3+} is discussed in several reports. For a critical evaluation of the stoichiometries and stability constants of the Al^{3+} complexes, see Martin (1986) and Bittar *et al.* (1992). At pH < 8, the predominant complex species is $[Al{\cdot}citH_{-1}]^-$, in which the citrate serves as a tridentate ligand with two carboxylates and a *deprotonated* hydroxy group. The ligand function of a deprotonated hydroxy group is strongly supported by X-ray crystallographic data on Al^{3+} complexes of hydroxy acids (Bombi *et al.*, 1990; van Koningveld & Venema, 1991; Feng *et al.*, 1990). The other species that, at high citric acid excesses, contributes to the complex equilibrium between pH 5 and 7.5 is $[Al{\cdot}cit_2]^{3-}$. The citric acid back-titration data on the NF peptides and phosphopeptides, featuring a C-terminal serine, suggest the adoption of a C-terminal type $[Al{\cdot}pepH_{-1}]^{-1}$ complex. In this *intramolecular* (intrachain) complex, the backbone is folded and the ligand groups are attached to a semicyclic peptide chain (Hollósi *et al.*, 1994). It is the stable, folded structure of the complex that prevents the extension of the chain and the formation of interchain complexes.

The use of TFE and other halogenated solvents, either as membrane mimetics or as an environment with helix-promoting ability, may be due to the duality of their low dielectric constants and high dipole moments (Jackson & Mantsch, 1992) [chloroethanol, ε = 25.8, D = 1.90; TFE, ε = 26.6 (Nelson & Kallenbach, 1986)]. Ethanol with ε = 25 and D = 1.71 has no helix-inducing effect. It is likely that the higher dipole moment of halogenated alcohols is responsible for unfolding of the peptide chain and refolding into an α-helical conformation. The CD spectra of phosphorylated and nonphosphorylated NF-M fragments have been found to have some helical character in TFE (Hollósi *et al.*, 1992; Ötvös *et al.*, 1988). The peptides, themselves, have no intrinsic potential to form β-pleated sheets. Thus, the α- to β-conformational transition is clearly the consequence of multivalent metal ion binding. The main role of TFE may be that it cannot solvate metal ions as effectively as water does, which likely increases the stability of the metal ion bridges. However, the relatively low dielectric constant may also stabilize the new system of H-bonds between the extended peptide chains. In TFE, Al^{3+} is expected to form more stable complexes with citric acid than in aqueous buffers. It follows from the failure of the citric acid back-titration experiments that the global log K_s values of $[Al{\cdot}pepH_{-1}]^{-1}$ type complexes in TFE are

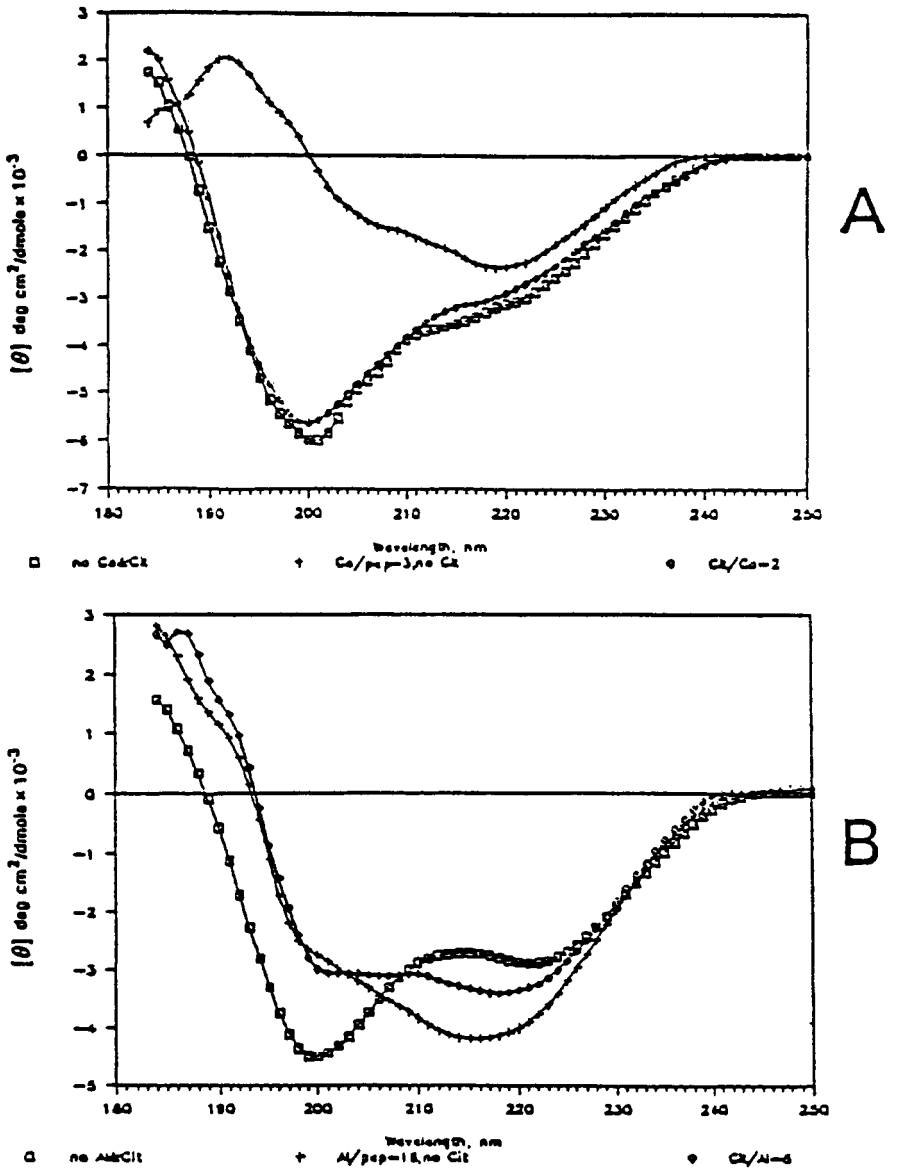

FIGURE 5: Citric acid back-titration of Ca^{2+} and Al^{3+}-induced conformational changes of NF-M17 for alanine-substituted peptides with citric acid in TFE: (A) NF-M17($A^1A^2A^{14}A^{15}$), [pep] = 0.343 mg/mL, □, no Ca^{2+} or citric acid, +, $[Ca^{2+}]/[pep] = 3$, ◇, $r_{Ca} = 3$ and $[cit]/[Ca^{2+}] = 2$; (B) NF-M17(A^6A^{11}), [pep] = 0.356 mg/mL, □, no Al^{3+} or citric acid, +, $[Al^{3+}]/[pep] = 16$, ◇, $r_{Al} = 16$ and $[cit]/[Al^{3+}] = 8$; concentration as in Figure 4.

likely higher than 8.1, which is the value of the $[Al{\cdot}citH_{-1}]^{-1}$ complex in water.

Al^{3+} titration data for NF-M17(A^6A^{11}) (Figure 2) and NF-M17(A^{11}) (Table 2) give strong support to the ligand function of the OH group in position 11. In models lacking this OH group, the *intrachain complex* cannot be formed. Instead, Al^{3+} ions cause chain extension and, most likely, the formation of the Al^{3+}-bridged β-pleated-sheet conformation. It is likely that the *N-terminal* EE...S^6 triad also has the ability for intrachain Al^{3+} complexation, but the stability of this complex likely is lower and it cannot prevent β-pleated-sheet formation at higher r_{Al} values.

The mono- and diphosphates of NF-M17-amide (Hollósi *et al.*, 1992) and NF-M13 were found to show β-pleated-sheet forming tendencies upon the binding of Ca^{2+} or Al^{3+} ions. Generally, a definite increase in the amount of β-pleated sheet was observed only at r_{Ca} and $r_{Al} > 5$. NF-M17(S^6P) [termed S^2P (Hollósi *et al.*, 1992)] also showed β-pleated-sheet capability. However, in concert with the data herein, the S^6P phosphopeptide was a weaker β-pleated-sheet former than its $S^{11}P$ isomer, lacking the C-terminal serine needed for the intrachain $[Al{\cdot}pepH_{-1}]$ type complex.

These findings, together with the Al^{3+} titration data for phosphopeptides of NF-M17($A^6S^{11}P$), -($A^{11}S^6P$), and -($S^{6,11}P$) (Table 1), support the existence of a second *interchain* $[Al^n{\cdot}pep_2]$ type of complex (n is the number of the possible binding sites along the peptide chain) (Hollósi *et al.*, 1994), which is formed with the participation of two or more peptide chains. This complex allows chain extension and further association of the β-pleated-sheet strands to form a complete β-pleated-sheet conformation. In the $[Al^n{\cdot}pep_2]$ type complex, which may correspond to the $[Al{\cdot}cit_2]^{3-}$ complex, the β-chains are cross-linked with Al^{3+} bridges. On the basis of the coordination chemistry of aluminum (Martin, 1986) and the X-ray crystallographic data for a trinuclear Al^{3+}–citrate complex featuring Al–O–Al bridges with the involvement of the deprotonated hydroxy group of citrate (Feng *et al.*, 1990), in the $[Al^n{\cdot}pep_2]$ type complex, Al^{3+} ions should have acidic (PO_3H^- and/or COO^-) ligands, but the formation of –O– bridges is also likely. The COO^- side chain groups of

contiguous glutamates (EE) are located above and below the average plane of a β-pleated sheet; therefore, the formation of an Al^{3+} bridge requires two anionic groups, one from each chain and one Al^{3+} per bridge. Thus, β-pleated-sheet formation may need up to five Al^{3+} ions per peptide in NF-M17, which has five anionic groups, and seven in NF-M17(S^6-$PS^{11}P$). This explains the observation that a >5 times excess of Al^{3+} is necessary to reach an r_{Al} value, above which no more β-pleated shift of the CD spectrum is observed. The complex equilibrium is described by the following equation:

$$2[Al{\cdot}pepH_{-1}] + (n-2)Al^{3+} \rightleftarrows [Al^{n}{\cdot}pep_2]$$

where n is the number of Al^{3+}-binding sites per peptide (the net charges are not shown). Aggregation of additional β-chains results in type $[Al^{mn}{\cdot}pep_m]$ *polycomplexes*, which stabilize β-sheets cross-linked by Al^{3+} bridges above and below the plane of the sheet. The CD titration data clearly show that, in the case of peptides with one (C-terminal) or two free serine residues, the type $[Al{\cdot}pepH_{-1}]$ intramolecular complex is preferred to the intermolecular ones formed between two anionic groups attached to different peptide chains.

The speculative models of intra- and intermolecular Al^{3+} complexes are in agreement with the CD-monitored Al^{3+} titration data shown in Figures 2, 4, and 5 and Table 1. The citric acid back-titrations indicate that, in TFE, both the intrachain and the interchain Al^{3+} complexes are stable enough to resist citric acid complexation.

One-dimensional ^1H NMR titrations of the NF-M17 peptide, in its unphosphorylated and phosphorylated forms, with Al^{3+} show broadening of the resonances and their coalescence toward a central frequency. Additionally, only 1–2 equiv of Al^{3+} have been added before precipitation of the peptide–metal complex begins to occur. These results are not promising for the extension to two-dimensional methods and full structural characterization of the ion-bound form. Comparative FT-IR spectroscopic studies of NF-M17 and NF-M17(A^6A^{11}) support the hypothesis of the formation of inter- and intramolecular Al^{3+} complexes (M. Hollósi, S. Holly, Z. M. Shen, and G. D. Fasman, manuscript in preparation).

To propose a rational explanation for Ca^{2+} complexation and Ca^{2+}-induced conformational transitions is indeed challenging. Ca^{2+} titration data on NF-M17(A^6A^{11}) showed that definite β-pleated-sheet formation occurs only if the molecule contains both serine residues (Figure 1, Table 1). Ca^{2+} has a more flexible ligand space (Bittar *et al.*, 1992; Martin, 1986) than does Al^{3+}. Moreover, in Ca^{2+} complexes an OH group does not play as important a role as it does in Al^{3+} complexes. The finding that in unphosphorylated NF-M13 (Hollósi *et al.*, 1992, 1993) and NF-M17, the spectral transition occurs at $r_{Ca} < 2$ may indicate that the major complex species is of the type $[Ca^{n}{\cdot}pep_2]$ (n = 1 or 2). The decrease in band intensities seen at $r_{Ca} > 2$ (Figure 1) is due to partial precipitation of the Ca^{2+} complex (Holly *et al.*, 1993; Hollósi *et al.*, 1992). This dimer may serve as a template for type $[Ca^{mn}{\cdot}pep_m]$ β-pleated-sheet polycomplexes, similar to the case of Al^{3+} complexes. The low r_{Ca} indicates that electrostatic forces also take part in assembling β-strands to form a β-pleated-sheet structure.

Secondary structural prediction showed that the KSPVPK-SP domain has practically no tendency to form a continuous β-pleated-sheet conformation (Ötvös *et al.*, 1988). This explains why the calculated amount of β-pleated-sheet conformation is usually below 50% (Table 3). Fourier transform infrared (FT-IR) spectroscopic studies on the Ca^{2+} complexes of phosphorylated NF-M17 fragments also showed the presence of significant amounts of unordered and other conformations in addition to the β-pleated sheet (Holly *et al.*, 1993). It is likely that the formation of Ca^{2+} cross-linked β-pleated-sheet segments is the cooperative result of favorable electrostatic, complexation, and structural effects. Contrary to Al^{3+}, Ca^{2+} does not have a tendency to form a folded type [Ca·pep] complex. If the $[Ca^{n}{\cdot}pep_2]$ type complex cannot be formed, the CD spectrum reflects a shift toward the unordered conformation (increased intensity and blue shift of the first $\pi\pi^*$ band). In the case of phosphorylated peptides, the spectral shift reflecting the β-pleated-sheet conformation occurs at higher r_{Ca} values, which may be taken as a sign of Ca^{2+} cross-linking between more than one pair of anionic COO^- and/or PO_3H^- groups. Finally, the surprising β-pleated-sheet formation by NF-M17($A^1A^2A^{14}A^{15}$), containing no COO^- groups, at $r_{Ca} > 2$ (supplementary material Figure 1C) may suggest that the major effect of the Ca^{2+} bridges in the glutamate models is due to the screening of the repulsion between the negatively charged groups.

The data discussed in this paper and in previous papers of the series (Hollósi *et al.*, 1992, 1993a,b, manuscript in preparation; Ötvös *et al.*, 1988) are believed to also have relevance to the dispute concerning the role of aluminum in the etiology of Alzheimer's disease and other neurodegenerative diseases that are marked by the accumulation of β-pleated-sheet aggregates. The comparable, or even higher, Al^{3+}-binding affinity in TFE of NF-M fragments, relative to that of citric acid, implies that the C-terminal acidic regions of the NF proteins may bind Al^{3+} with high log K_s values, even in the natural environment of neurons. However, if the Al^{3+} complex is of the type $[Al{\cdot}pepH_{-1}]$, then the folded structure does not allow the adoption of the β-pleated-sheet conformation.

The C-terminal tail of NF-M proteins has more flexibility than the triple-helical N-terminal head domain. It can probably easily tolerate the conformational effect that is caused by intrachain complexation. The major problem is that the intrachain complex is very stable, and the bound Al^{3+} may have a long-lasting effect.

Further accumulation of Al^{3+}, phosphorylation, aberrant degradation, and other factors that also play an essential role in the etiology of AD may, however, lead to the $[Al{\cdot}pepH_{-1}] \rightarrow [Al^{n}{\cdot}pep_2] \rightarrow [Al^{mn}{\cdot}pep_m]$ shifts of the complex equilibria and trigger the β-aggregation process. In the $[Al^{n}{\cdot}pep_2]$ complex, the neighboring chains already have at least a partially parallel or antiparallel β-orientation. Thus, even a short $[Al^{n}{\cdot}pep_2]$ double-stranded β-pleated-sheet segment may serve as a *seed* for β-aggregation in a process that resembles crystallization. The β-aggregates may also be formed from different proteins (or their proteolytic fragments). The Al^{3+} bridges may also be effective in binding acidic components (e.g., acidic proteoglycans) (Tokutake, 1990; Selkoe *et al.*, 1979), as well as causing different β-filaments to associate. Ca^{2+} ions, due to their lower affinity toward fragments having the same COO^-, PO_3H^-, and OH ligand groups, are less effective. Ca^{2+} is involved in the delicate ion equilibria in the cytosol, and a complexation of Ca^{2+}, which induces β-aggregation, requires long-lasting pathological or age-related exposure to high Ca^{2+} levels. Al^{3+} is a more effective aggregating agent due to the higher stabilities of its intra- and intermolecular complexes. The strong and/or long-lasting complexation of Al^{3+} places emphasis on the importance of dietary factors (aluminum intake by drinking water or other liquids, foods, and drugs) in consideration of the prevention

or retardation of Alzheimer's disease and other aluminum-related neurodegenerative diseases.

ACKNOWLEDGMENT

We thank Dr. Cathy Moore for the NMR results.

SUPPLEMENTARY MATERIAL AVAILABLE

Figures illustrating the circular dichroism titration of NF-M17 in TFE with Ca^{2+} (Figure 1), circular dichroism titration of NF-M17 in TFE with Al^{3+} (Figure 2), citric acid back-titration experiments on the Ca^{2+} complexes of NF-M13 phosphorylated derivatives in TFE (Figure 3), citric acid back-titration experiments on the Al^{3+} complexes of NF-M13 phosphorylated derivatives in TFE (Figure 4), and citric acid back-titration of Ca^{2+}- and Al^{3+}-induced conformational changes in NF-M17 for alanine-substituted peptides with citric acid in TFE (Figure 5) (9 pages). Ordering information is given on any current masthead page.

REFERENCES

Biernat, J., Mandelkow, E.-M., Schröter, C., Lichtenberg-Kraag, B., Steiner, B., Berling, B., Meyer, H., Mercken, M., Vandermeeren, A., Goedert, M., & Mandelkow, E. (1992) *EMBO J. 11*, 1593–1597.

Bittar, E. E., Xiang, Z., & Huang, Y.-P. (1992) *Biochim. Biophys. Acta 1108*, 210–214.

Bombi, G. G. Corain, B., & Sheikh-Osman, A. A. (1990) *Inorg. Chim. Acta 171*, 79–83.

Crapper, D. R., & Dalton, A. J. (1973) *Physiol. Behav. 10*, 935–945.

Crapper-McLachlan, D. R. (1986) *Neurobiol. Aging 7*, 525–532.

Crapper-McLachlan, D. R., & Van Berkum, F. A. (1986) *Prog. Brain Res. 70*, 399–408.

Delamarche, C. (1989) *Biochimie 71*, 853–856.

Doll, R. (1993) *Age Ageing 22*, 138–153.

Feng, T. L., Gurian, P. L., Healey, M. D., & Barron, A. R. (1990) *Inorg. Chem. 29*, 208–411.

Fields, G. B., & Noble, R. L. (1990) *Int. J. Pept. Protein Res. 35*, 161–214.

Geisler, N., Kaufmann, E., Fischer, S., Plessmann, U., & Weber, K. (1983) *EMBO J. 2*, 1295–1302.

Hollósi, M., Ürge, L., Perczel, A., Kajtár, J., Teplan, I., Ötvös, L., Jr., & Fasman, G.D. (1992) *J. Mol. Biol. 223*, 673–682.

Hollósi, M., Ötvös, L., Jr., Ürge, L., Kajtár, J., Perczel, A., Laczkó, I., Vadász, Zs., & Fasman, G. D. (1993) *Biopolymers 33*, 497–510.

Hollósi, M., Shen, Z. M., Perczel, A., & Fasman, G. (1994) *Proc. Natl. Acad. Sci. U.S.A. 91*, 4902–4906.

Holly, S., Laczkó-Hollósi, I., Fasman, G. D., & Hollósi, M. (1993) *Biochem. Biophys. Res. Commun. 197*, 755–762.

Jackson, M., & Mantsch, H. H. (1992) *Biochim. Biophys. Acta 1118*, 139–143.

Kennedy, M. B. (1989) *Trends Neurosci. 12*, 417–420.

Khachaturian, Z. S. (1989) *Aging 1*, 17–34.

Klatzo, I., Wisniewski, H. M., & Streicher, E. (1965) *J. Neuropathol. Exp. Neurol. 24*, 187–210.

Landsberg, J. P., McDonald, B., & Watt, F. (1992) *Nature 360*, 65–68.

Leterrier, J. F., Langui, D., Probst, A., & Ulrich, J. (1992) *J. Neurochem. 58*, 2060–2070.

Martin, R. B. (1986) *J. Inorg. Biochem. 28*, 181–187.

Meiri, H., Banin E., Roll, M., & Rousseau, A. (1993) *Prog. Neurobiol. 40*, 89–121.

Myers, M. W., Lazzarini, R. A., Lee, V. M.-Y., Schlaepfer, W. W., & Nelson, D. L. (1987) *EMBO J. 6*, 1617–1626.

Nelson, J. W., & Kallenbach, N. R. (1986) *Proteins: Struct., Funct., Genet. 1*, 211–217.

Ötvös, L., Jr., Hollósi, M., Perczel, A., Dietzschold, B., & Fasman, G. D. (1988) *J. Protein Chem. 7*, 365–376.

Ötvös, L., Jr., Tangoren, I. A., Wroblewski, K., Hollósi, M., & Lee, V. M.-Y. (1990) *J. Chromatogr. 512*, 265–272.

Perczel, A., Park, K., & Fasman, G. D. (1992) *Anal. Biochem. 203*, 83–93.

Perl, D. P., Gajdusek, D. C., Garruto, R. M., Yanagihara, R. T., & Gibbs, C. J., Jr. (1982) *Science 217*, 1053–1055.

Perry, G. (1990) in *Neuro-Science Year* (Smith, B., & Adelman, G., Eds.) pp 5–8, Birkhäuser, Boston.

Prevelige, P., Jr., & Fasman, G. D. (1987) *Biochemistry 26*, 2944–2955.

Saito, K.-I., Elce, J. S., Hamos, J. E., & Nixon, R. A. (1993) *Proc. Natl. Acad. Sci. U.S.A. 90*, 2628–2632.

Selkoe, D. J. (1991) *Neuron 6*, 487–498.

Selkoe, D. J., Liem, R. K. H., Yen, S. H., & Shelanski, M. L. (1979) *Brain Res. 163*, 235–252.

Terry, R. D., & Pena, C. (1965) *J. Neuropathol. Exp. Neurol. 24*, 200–210.

Tokutake, S. (1990) *Int. J. Biochem. 22*, 1–6.

van Koningsveld, H., & Venema, F. R. (1991) *Acta Crystallogr. C47*, 289–292.

Wisniewski, H., Karczewski, W., & Wisniewski, R. (1966) *Acta Neuropathol. 6*, 211–219.

Zékány, L., & Nagypál, I. (1985) in *Computational Methods for the Determination of Formation Constants* (Leggett, D. J., Ed.) Chapter 8 (PSEQUAD), Plenum Press, New York.